Environmental Pollution 185 (2014) 59–68

Contents lists available at ScienceDirect

Environmental Pollution

journal homepage: www.elsevier.com/locate/envpol

# Coal-tar-based sealcoated pavement: A major PAH source to urban stream sediments

Amy E. Witter [a,*], Minh H. Nguyen [a,1], Sunil Baidar [a,2], Peter B. Sak [b]

[a] Department of Chemistry, Dickinson College, PO Box 1773, Carlisle, PA 17013, USA
[b] Department of Earth Sciences, Dickinson College, PO Box 1773, Carlisle, PA 17013, USA

ARTICLE INFO

*Article history:*
Received 4 July 2013
Received in revised form
8 October 2013
Accepted 11 October 2013

*Keywords:*
Sediment
Coal-tar-based sealcoat
Polycyclic aromatic hydrocarbons
Urban sprawl
Streams
Land use

ABSTRACT

We used land-use analysis, PAH concentrations and assemblages, and multivariate statistics to identify sediment PAH sources in a small (~1303 km$^2$) urbanizing watershed located in South-Central, Pennsylvania, USA. A geographic information system (GIS) was employed to quantify land-use features that may serve as PAH sources. Urban PAH concentrations were three times higher than rural levels, and were significantly and highly correlated with combined residential/commercial/industrial land use. Principal components analysis (PCA) was used to group sediments with similar PAH assemblages, and correlation analysis compared PAH sediment assemblages to common PAH sources. The strongest correlations were observed between rural sediments ($n = 7$) and coke-oven emissions sources ($r = 0.69–0.78$, $n = 5$), and between urban sediments ($n = 22$) and coal-tar-based sealcoat dust ($r = 0.94$, $n = 47$) suggesting that coal-tar-based sealcoat is an important urban PAH source in this watershed linked to residential and commercial/industrial land use.

© 2013 Elsevier Ltd. All rights reserved.

## 1. Introduction

Recent evidence indicates that coal-tar-based pavement sealant is a major source of particulate polycyclic aromatic hydrocarbons (PAHs) in urban waterways, especially in the central and eastern U.S. (Mahler et al., 2005; Van Metre et al., 2009; Van Metre and Mahler, 2010). PAHs are byproducts of both fossil-fuel combustion and petrogenic sources, and they are of special toxicological and environmental concern due to their carcinogenic potential (U.S. EPA, 1993). Urban freshwater sediments serve as PAH repositories due to the intensity of human activities (e.g. driving, habitation) that occur in these areas, as well as from land-use changes resulting from increased urbanization. Urban land-use change increases the amount of impervious surface cover, which facilitates greater surface runoff, a major PAH transport pathway in the environment (Hoffman et al., 1984).

Geographic information systems (GIS) in conjunction with chemical measurements can be used to identify and quantify land-use features associated with pollutants in order to predict chemical distributions and impacts. For instance, Comeleo et al. (1996) used GIS in combination with principal components analysis (PCA), rank correlation analysis, and multiple linear regression (MLR) modeling to link the percentage of developed land in 25 estuarine subwatersheds located in Chesapeake Bay with PAH sediment concentrations. In a later study, Paul et al. (2002) expanded on this earlier work by including 75 small estuaries extending over a larger region of the mid-Atlantic and southern New England and again found a positive correlation between total PAHs and percent urban land use. More recently, Chalmers et al. (2007) evaluated the relationship between urbanization and PAH concentrations in surface sediments and sediment cores in New England and found that PAH concentrations were strongly correlated with urbanization, in particular with the percentage of commercial, industrial, and transportation land use. Other studies have shown strong correlations between urban land-use metrics and PAH concentrations in storm water (Jartun et al., 2008), wetlands (Crosbie and Chow-Fraser, 1999), and moss biomonitors (Augusto et al., 2011) emphasizing that land-use activities influence PAH concentrations in urban ecosystems.

Although GIS is widely used for monitoring, assessment, and management purposes, efforts to develop robust, predictive relationships between specific urban land-use metrics and resulting sediment PAH impacts are complicated. Questions that remain poorly understood in its use are: What are the most relevant urban

* Corresponding author.
*E-mail addresses:* witter@dickinson.edu (A.E. Witter), sakp@dickinson.edu (P. B. Sak).
[1] Current address: Department of Chemistry, University of Pennsylvania, Philadelphia, PA 19104, USA.
[2] Current address: Department of Chemistry and Biochemistry, University of Colorado Boulder, Boulder, CO 80309, USA.

0269-7491/$ – see front matter © 2013 Elsevier Ltd. All rights reserved.
http://dx.doi.org/10.1016/j.envpol.2013.10.015

land-use features that predict the impact of nonpoint source pollution? Over what spatial scales do these operate? What PAH sources are associated with specific urban land-use features? To better understand and explain the mechanistic connection between urbanization and increasing sediment PAH concentrations requires that functional linkages be established between urban land-use activities and unique chemical signatures reflecting those activities (Riva-Murray et al., 2010).

In the present study we investigated the influence of urban land use on sediment PAH concentrations and assemblages in the Conodoguinet Creek, a small urbanizing watershed located in south-central Pennsylvania, USA. Although it is a small watershed, the Conodoguinet Creek provides significant economic and societal services within the region that typify many other small watersheds located throughout the U.S., and may serve as a model for areas undergoing similar land-use changes. We hypothesized urban sediments would show higher PAH concentrations than rural sediments, and that chemical measurements combined with multivariate statistics could help identify major PAH sources in the watershed.

## 2. Materials and methods

### 2.1. Study area

The Conodoguinet Creek watershed drains a 1303 km$^2$ area throughout Cumberland County, PA with its headwaters located in Franklin County, PA (Fig. 1). The 167-km stream flows west to east through diverse landscapes including forests, agricultural areas, interstate highways, small towns and urban centers, before emptying into the Susquehanna River in Harrisburg, PA. The creek serves as a major source of drinking water for the region, with communities in the eastern end of the Cumberland Valley withdrawing over 8 million gallons per day for residential and commercial purposes (Alliance for Chesapeake Bay, 1994). Two interstate highways and the Pennsylvania Turnpike pass through the Cumberland Valley, and Carlisle, PA serves as a major trucking hub and distribution center for the Atlantic Coast. Consequently, as the Conodoguinet Creek flows eastward from its headwaters to the Susquehanna River, it transits an increasingly urbanized land-use gradient.

### 2.2. Sample collection

Streambed surface sediment samples were collected from 35 sites within the Conodoguinet Creek watershed during May 2010. The creek was roughly divided into thirty-five, 5-km segments from which sediments were collected. In some instances, access to the stream prohibited evenly-spaced sampling; in those instances, samples of opportunity were collected. The sampling protocol targeted depositional zones with organic carbon-rich sediment where possible, and avoided areas directly adjacent to known point sources. At each sampling site, 5 grab samples were collected with a stainless steel scoop from depositional zones along a 25-m length of stream, and were combined together in a stainless steel bowl to make up a composite sample. Then, a 50 g portion of the composite sample was removed and placed in a solvent-rinsed amber glass jar with Teflon cap. Based on the sample collection depth (1–2 cm), the sediments are expected to represent modern inputs. All samples were transported on ice to the laboratory, and were freeze-dried to remove residual water. After drying, the samples were sieved through a 1-mm sieve (ASTM No. 18) to obtain a consistent particle size for extraction. Visible debris such as sticks or gravel was removed before sieving. The sieved samples were returned to the collection jars and stored frozen at −20 °C until analysis.

### 2.3. Analytical methods

Sediments were extracted in dichloromethane using accelerated solvent extraction (ASE), cleaned using solid-phase extraction (SPE) chromatography, and analyzed for 19 PAHs ($\sum PAH_{19}$) including: naphthalene (Naph), 2-methylnaphthalene (2-Naph), acenaphthylene (Acy), acenapthene (Ace), fluorene (Flu), phenanthrene (Phe), anthracene (Anth), fluoranthene (Fla), pyrene (Py), benz[*a*]anthracene (BaA), chrysene (Chry), benzo[*b*]fluoranthene (BbF), benzo[*k*]fluoranthene (BkF), benzo[*j*]fluoranthene (BjF), benzo[*e*]pyrene (BeP), benzo[*a*]pyrene (BaP), indeno[*1,2,3-cd*]pyrene (Ip), dibenz[*a,h*]anthracene (DBA), and benzo[*ghi*]perylene (BghiP) via gas chromatography/mass spectrometry (GC/MS) operated in single-ion monitoring (SIM) mode. Although 19 PAHs were measured, 12 parent PAHs were summed for further statistical tests because they were frequently (≥98%) detected in these sediment samples, and they are consistently included in many published source profiles. The 12 PAHs are phenanthrene (Phe), anthracene (Anth), fluoranthene (Fla), pyrene (Py), benz[*a*]anthracene (BaA), chrysene (Chry), benzo[*b*]fluoranthene (BbF), benzo[*k*]fluoranthene (BkF), benzo[*e*]pyrene (BeP), benzo[*a*]pyrene (BaP), indeno[*1,2,3-cd*]pyrene (Ip), and benzo[*ghi*]perylene (BghiP). Consequently, $\sum PAH_{12}$ is the sum of these 12 PAHs. Additional information on analytical methods and quality assurance/quality control (QA/QC) are provided in the Supplementary information.

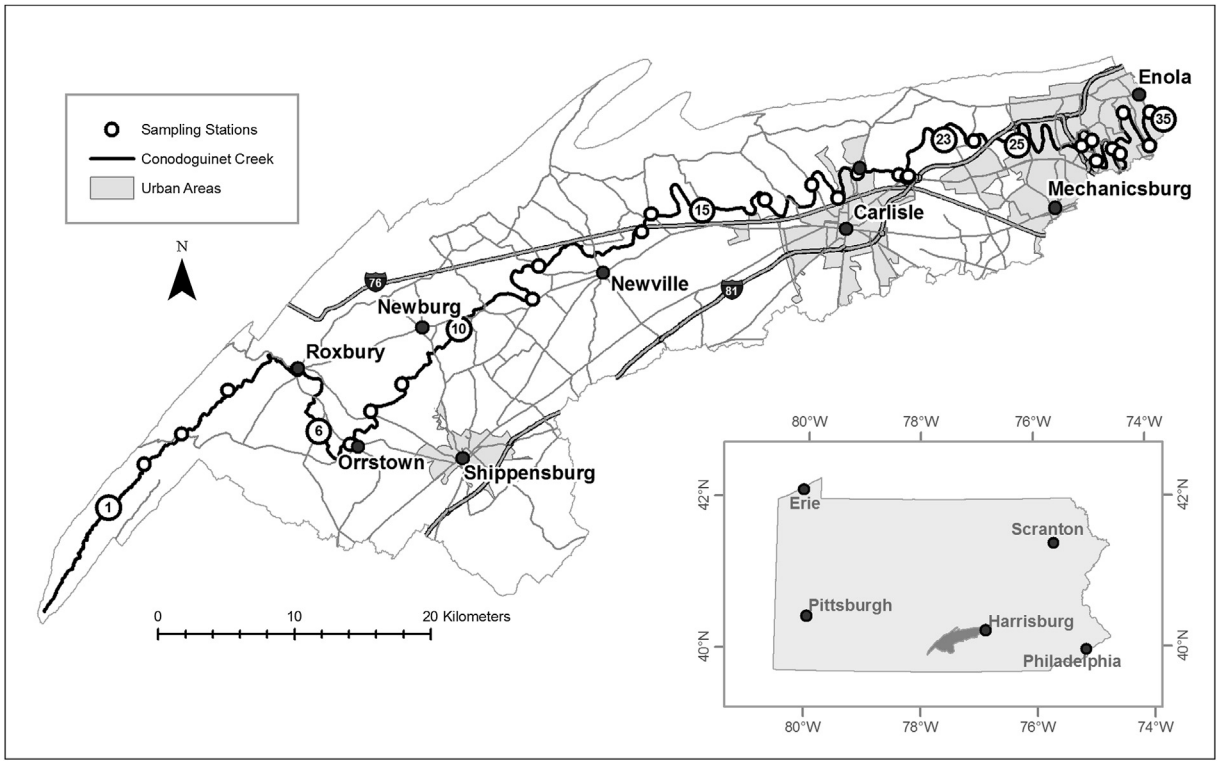


**Fig. 1.** Map of the Conodoguinet Creek watershed, PA, USA, with selected sites annotated for reference.

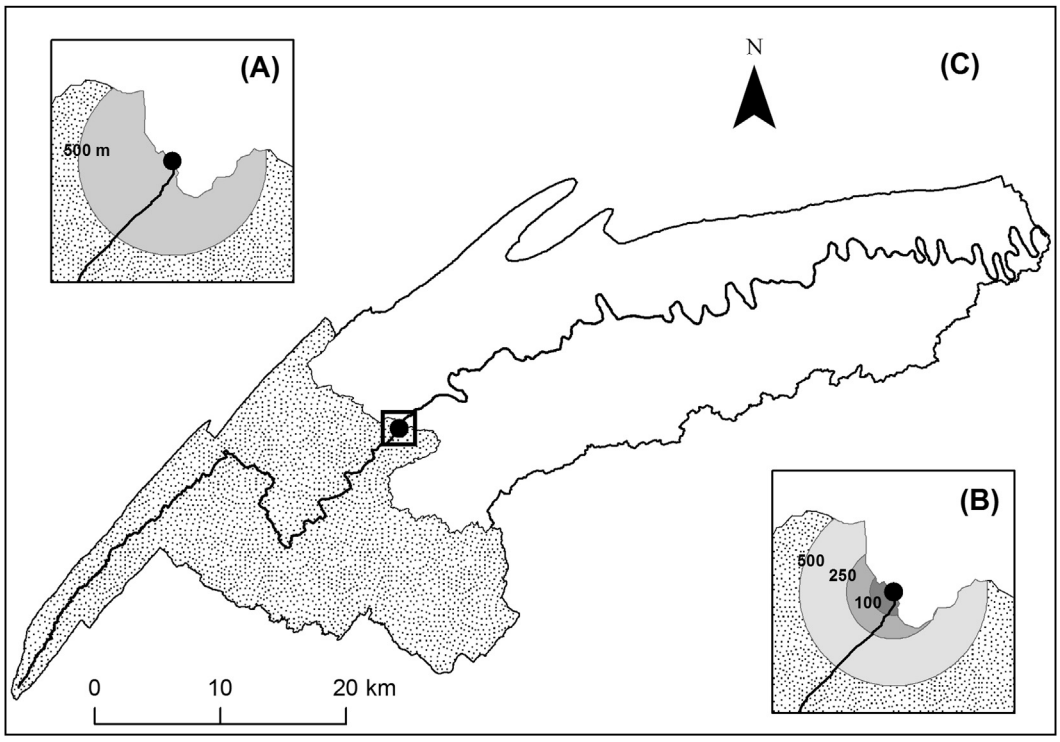


**Fig. 2.** Illustration showing how the GIS spatial scales described in the text were calculated. (A) 500-m upstream buffer. Land use/land cover within 500-m upstream of the sampling site was quantified with equal weight given to each class within the buffer area; (B) 500-m inverse-distance-weighted (IDW) upstream buffer. Land use/land cover within 500-m upstream of the sampling site was quantified with greater weight given to land use/land cover located closer to sampling site (within 0–100 m; dark gray circle) than land located farther away (250–500 m; light gray circle); (C) integrated upstream watershed area. Land use/land cover was calculated including the integrated upstream area from each sampling site. Buffers are not drawn to scale. Distances represented on the map buffers are measured in meters.

### 2.4. Spatial analysis

Watershed boundaries around each sampling site were delineated using a 1:24,000 digital elevation model (DEM) expressed as a 10–m raster (USGS National Elevation Data Set, www.usgs.gov). A raster mosaic containing the stream was created and projected into Pennsylvania State Plane. Thirty-five individual sub-watersheds within the basin were delineated based on GPS locations of the sampling sites. Impervious surface area data were obtained from the USGS (National Land Cover Data, 2006 Percent Developed Imperviousness) and were calculated on a pixel-by-pixel basis. Land cover data were obtained from PAMAP Program Land Cover for Pennsylvania, 2005 (Available FTP: http://www.pasda.psu.edu). Thirty-seven land-use classifications in the original PAMAP data were downsampled to 15 land-use categories. For example, the three types of forested land use (deciduous, evergreen, and mixed deciduous and evergreen) in the source data were binned into a single forested category. The fifteen new land cover categories included: roads, agriculture, forested, water, wetlands, bare land, low-, mid- and high-residential and commercial land, airports, golf courses, and mines. In some instances, land-use categories present in the original dataset (i.e. mines) were not present in the study area.

For the purposes of further statistical analyses, five urban land-use categories (CIR, RES, URB, RESCI, RDS; described below) and one land-cover category (IMP) were calculated. In this study, *land-use* refers to the economic uses of land within the watershed (i.e. for residential, commercial, industrial purposes, etc.) while *land cover* refers to the physical features that cover the land (i.e. impervious surface). Consequently, parcels of land may have similar land cover but may be used for different economic purposes. The land-use/land-cover categories include: 1) percentage impervious surface area (IMP), defined as the sum across all pixels of the fraction of impervious surface in each pixel; 2) percentage commercial/industrial land & roads (CIR), defined as the sum of low-, mid- and high-density commercial land area plus the sum of the state-road area divided by the sub-watershed area × 100%; 3) percentage residential land (RES), defined as the sum of low-, mid- and high-density residential land area divided by the sub-watershed area × 100%; 4) percentage urban land (URB), defined as the sum of low-, mid- and high-density residential land area (RES) and commercial land area plus the sum of the state road area (CIR) divided by the sub-watershed area × 100%; 5) percentage residential & commercial/industrial land (RESCI), defined as the sum of low-, mid- and high-density residential land area (RES) and commercial/industrial land area divided by the sub-watershed area × 100%; and 6) percentage roads (RDS), defined as the sum of state road area divided by the sub-watershed area × 100%.

Land-use parameters were measured at three spatial scales including 500-m circular upstream buffers, 500-m inverse-distance-weighted upstream buffers, and over the integrated upstream watershed (Fig. 2A–C). Circular upstream buffers centered at each sampling site were drawn with radii of 500 m, and the areas occupied by each land use class contained in each buffer area were computed (Fig. 2A). Only the land use area contained upstream of the sampling site was considered in our calculation because flow is unidirectional; once the creek flow was downstream of the sampling site, it would not further influence the PAH concentration of an upstream site. This approach takes into account the landscape topology when quantifying land-use influence within a specified distance from the sampling site.

Inverse-distance weights were applied to each of the six urban land-use/land-cover categories defined above to test the hypothesis that urbanized land proximate to the stream would have a larger influence on total PAHs then land located farther away. Linear distances (m) were calculated between each cell and the stream for urban land-use/land-cover cell types in the watershed (i.e. impervious surface, residential, commercial, and roads). Counts of distances were aggregated into unequal interval distance classes: 0–100 m, 101–200 m, 201–500 m, 501–1000 m, and 1001–2500 m. The highest distance in each range was used to represent all cells within the range. One inverse-distance weight ($d^{-1}$) was applied to all land-cover cells within each range, and the percentage of each weighted-land type was calculated by dividing the number of each distance-weighted cell of a particular type (i.e. residential) by the total number of distance-weighted cells within each distance class × 100%. Then, circular upstream buffers centered at each sampling location were again drawn with radii of 500 m, and the upstream area occupied by each weighted land-use class contained within the buffer was computed (Fig. 2B).

The integrated upstream watershed approach sums all land-use categories located upstream of a sampling site together to comprise the integrated upstream area. This approach (Fig. 2C) assumes that all pixels of a specific land-use type contribute equally to sediment contamination, regardless of distance from the site.

### 2.5. Correlation analysis

Three correlation approaches were used to evaluate relationships between variables in this study. First, six urban land-use/land-cover metrics and $\Sigma PAH_{12}$ for $n = 34$ sites were correlated using Spearman's rank correlation method (site 5 was not included in this analysis due to high standard residuals). Rank-transformation methods are useful for correlating non-normally distributed data (Conover and Iman, 1981), such as the $\sum PAH_{12}$ reported in this study, which showed higher

**Table 1**
Concentrations (in μg $kg^{-1}$ dry weight) of 19 PAHs measured in 35 Conodoguinet Creek sediments.

| Site# | Naph | 2-Naph | Acy | Ace | Flu | Phe | Anth | Fla | Py | BaA | Chry | BbF | BkF | BjF | BeP | BaP | DBA* | Ip | BghiP | Total PAHs |
|---|---|---|---|---|---|---|---|---|---|---|---|---|---|---|---|---|---|---|---|---|
| 0 | nd | nd | nd | nd | nd | nd | nd | nd | nd | nd | nd | 5 | nd | nd | nd | nd | 16 | 14 | 10 | 44 |
| 1 | 47 | 12 | nd | nd | nd | 6 | nd | nd | nd | nd | nd | 2 | nd | nd | nd | nd | 10 | 9 | 6 | 91 |
| 2 | 70 | 17 | nd | nd | nd | 12 | nd | 52 | 47 | 23 | 12 | 101 | 28 | 28 | 103 | 43 | 38 | 25 | 31 | 628 |
| 3 | 78 | 19 | 18 | nd | nd | 26 | 20 | 194 | 204 | 129 | 105 | 613 | 279 | 272 | 479 | 131 | 107 | 55 | 69 | 2798 |
| 4 | 75 | 18 | nd | nd | nd | 12 | nd | 35 | 27 | 8 | 3 | 336 | 94 | 94 | 396 | 40 | 84 | 49 | 72 | 1342 |
| 5 | 113 | 39 | 287 | 171 | 241 | 1377 | 243 | 2752 | 2392 | 1131 | 1106 | 4394 | 2133 | 2064 | 3861 | 1445 | 720 | 702 | 1054 | 26,226 |
| 6 | 79 | 20 | 13 | nd | nd | 75 | 11 | 143 | 139 | 58 | 58 | 139 | 64 | 57 | 134 | 82 | 31 | 40 | 57 | 1198 |
| 7 | 109 | 21 | 5 | nd | nd | 54 | 8 | 98 | 92 | 28 | 33 | 144 | 50 | 52 | 151 | 60 | 37 | 34 | 49 | 1025 |
| 8 | 41 | 5 | 38 | nd | 4 | 312 | 61 | 870 | 691 | 320 | 332 | 1589 | 770 | 738 | 1345 | 392 | 261 | 162 | 224 | 8153 |
| 9 | 15 | 6 | 36 | nd | nd | 199 | 40 | 328 | 303 | 149 | 144 | 176 | 79 | 80 | 159 | 176 | 40 | 109 | 131 | 2172 |
| 10 | 10 | 4 | 29 | nd | nd | 199 | 41 | 371 | 329 | 150 | 179 | 242 | 107 | 97 | 213 | 200 | 48 | 130 | 161 | 2509 |
| 11 | 9 | 2 | 17 | nd | nd | 69 | 15 | 133 | 136 | 57 | 63 | 126 | 46 | 51 | 121 | 82 | 31 | 54 | 69 | 1080 |
| 12 | 8 | 3 | 27 | nd | nd | 78 | 20 | 176 | 165 | 70 | 70 | 178 | 69 | 78 | 157 | 91 | 35 | 58 | 73 | 1355 |
| 13 | 11 | 5 | 20 | nd | nd | 70 | 13 | 139 | 146 | 55 | 69 | 175 | 71 | 84 | 172 | 82 | 38 | 51 | 65 | 1267 |
| 14 | 13 | 10 | 21 | nd | nd | 57 | 14 | 134 | 148 | 50 | 77 | 359 | 139 | 161 | 355 | 88 | 77 | 58 | 75 | 1835 |
| 15 | 15 | 8 | 37 | nd | nd | 113 | 36 | 228 | 250 | 108 | 126 | 165 | 73 | 74 | 160 | 142 | 37 | 85 | 109 | 1765 |
| 16 | nd | nd | 8 | nd | nd | 76 | 12 | 167 | 203 | 81 | 93 | 70 | 27 | 27 | 70 | 89 | 18 | 50 | 59 | 1050 |
| 17 | 10 | 3 | 55 | 9 | 30 | 452 | 78 | 721 | 601 | 238 | 250 | 241 | 118 | 111 | 202 | 275 | 48 | 168 | 200 | 3809 |
| 18 | 19 | 11 | 68 | nd | nd | 105 | 65 | 262 | 285 | 147 | 135 | 149 | 64 | 66 | 135 | 157 | 34 | 106 | 125 | 1934 |
| 19 | 8 | 10 | 26 | nd | nd | 195 | 34 | 452 | 373 | 189 | 226 | 263 | 120 | 107 | 218 | 242 | 51 | 172 | 200 | 2886 |
| 20 | 12 | 7 | 38 | nd | nd | 126 | 46 | 332 | 307 | 146 | 165 | 188 | 83 | 81 | 166 | 185 | 39 | 134 | 160 | 2215 |
| 21 | 91 | 55 | 312 | 43 | 69 | 1129 | 412 | 2150 | 2038 | 1005 | 1235 | 965 | 538 | 530 | 970 | 1116 | 259 | 856 | 1062 | 14,833 |
| 22 | 39 | 32 | 151 | 4 | 21 | 504 | 181 | 1119 | 1051 | 478 | 610 | 509 | 267 | 265 | 493 | 565 | 142 | 398 | 499 | 7329 |
| 23 | 18 | 8 | 104 | 6 | 16 | 488 | 205 | 1239 | 1070 | 621 | 555 | 459 | 248 | 230 | 398 | 564 | 124 | 343 | 389 | 7086 |
| 24 | 14 | 10 | 56 | nd | 2 | 189 | 72 | 509 | 463 | 247 | 275 | 250 | 118 | 109 | 226 | 263 | 67 | 187 | 224 | 3281 |
| 25 | 31 | 27 | 186 | nd | 10 | 431 | 241 | 1132 | 1101 | 611 | 1019 | 554 | 288 | 264 | 537 | 621 | 146 | 423 | 532 | 8154 |
| 26 | 13 | 9 | 65 | nd | nd | 173 | 70 | 435 | 418 | 202 | 228 | 219 | 110 | 101 | 207 | 234 | 66 | 176 | 213 | 2940 |
| 28 | 30 | 21 | 126 | 4 | 21 | 436 | 186 | 943 | 902 | 443 | 452 | 401 | 193 | 183 | 377 | 449 | 106 | 304 | 364 | 5942 |
| 29 | 19 | 13 | 68 | 3 | 11 | 324 | 97 | 809 | 705 | 346 | 419 | 396 | 201 | 185 | 359 | 391 | 102 | 296 | 352 | 5094 |
| 30 | 31 | 22 | 149 | 4 | 18 | 423 | 187 | 980 | 964 | 493 | 478 | 407 | 208 | 194 | 374 | 489 | 105 | 307 | 363 | 6196 |
| 31 | nd | 7 | 72 | nd | 4 | 280 | 71 | 711 | 618 | 284 | 375 | 387 | 184 | 179 | 345 | 335 | 93 | 271 | 324 | 4541 |
| 32 | 17 | 9 | 70 | nd | 2 | 252 | 89 | 731 | 638 | 330 | 380 | 370 | 178 | 172 | 326 | 376 | 92 | 270 | 321 | 4623 |
| 33 | 28 | 54 | 75 | 22 | 34 | 613 | 133 | 1287 | 1053 | 537 | 604 | 546 | 289 | 257 | 477 | 558 | 125 | 401 | 466 | 7558 |
| 34 | 2 | nd | 24 | 3 | 11 | 387 | 57 | 882 | 674 | 316 | 380 | 346 | 175 | 162 | 286 | 345 | 79 | 238 | 268 | 4635 |
| 35 | 42 | 42 | 216 | 43 | 48 | 893 | 282 | 1842 | 1676 | 835 | 828 | 834 | 477 | 396 | 779 | 906 | 193 | 646 | 806 | 11,785 |

*DBA isomers not resolved by GC column.

concentrations in urban versus rural areas. After transforming the PAH concentration data into ranked data, Spearman's rho ($\rho$), a nonparametric measure of the statistical dependence between two variables, was calculated.

The Chi-square statistic ($X^2$) was used to compare similarities in PAH distributions between rural and urban sediment PAH profiles measured in this study and seven putative PAH source profiles compiled from the literature. This nonparametric statistic was calculated as the square of the difference in proportional PAH concentrations divided by the mean of the two values, summed for the 12 PAHs (Van Metre and Mahler, 2010). The lower the $X^2$ value, the more similar are the two profiles. Pearson's correlation coefficient ($r$), a parametric measure of the linear dependence between variables, was also calculated for comparative purposes in each case, as it was assumed that if a correlation was observed, it might provide additional information on potential PAH sources.

### 2.6. Statistical analyses

Principal components analysis (PCA) was used to group sediments exhibiting similar chemistry using Solo software (Eigenvector Research, Inc., Wenatchee, WA). Fractional concentrations of 12 individual PAH compounds in each sediment sample were calculated by dividing the concentrations of individual PAH compounds by the total $\sum PAH_{12}$ concentration (e.g. $PAH_i/\sum PAH_{12}$) to minimize concentration variability between sites (Dickhut et al., 2000; Zheng et al., 2011). Data from three sites were not included in the analysis (sites 0, 1, and 5) because there were non-detectable concentrations (sites 0, 1) or because of the unusually high standard residuals (site 5). Data subjected to PCA analysis consisted of a matrix of 32 sediment samples and 12 PAHs (384 data points).

## 3. Results and discussion

### 3.1. Spatial distribution of PAHs/land use in the Conodoguinet Creek watershed

Total concentrations for 19 PAHs ($\sum PAH_{19}$) in 35 surface sediments ranged from 44 μg $kg^{-1}$ to 26,200 μg $kg^{-1}$ with a mean and median concentration of 4100 and 2280 μg $kg^{-1}$, respectively (Table 1). In general, urban sediments collected from the eastern end of the watershed had PAH concentrations that were approximately three times greater than sediments collected from rural western areas (Fig. 1). An exception to this trend was observed at site 5, which had the highest PAH concentration measured in the watershed ($\sum PAH_{19}$ = 26,200 μg $kg^{-1}$). Sediment from site 5 was enriched in BbF, BkF, and BeP relative to other isomers; however, the PAH source identity could not be unambiguously identified based on its fractional PAH assemblage. Interestingly, site 5 was also anomalous in terms of its land use/land-cover characteristics, which were typical of more highly urbanized sites located in the eastern end of the watershed (Table 2). The remainder of the PAH concentrations measured throughout the watershed fell below the probable effect concentration (PEC) of 22,800 μg $kg^{-1}$ established for nine PAH isomers ($\sum$Anth + Flu + Napt + Phe + BaP + BaA + Chry + Fla + Py) by MacDonald et al. (2000).

To aid in identifying PAH sources associated with specific urban land-use features, we used a geographic information system (GIS) to quantify five land-use categories (CIR, RES, URB, RESCI, and RDS) and one land-cover category (IMP) within the watershed (Table 2). Because the spatial scale that best predicts chemical impacts may vary for different pollutants based on physical–chemical properties, we examined land-use buffers at three spatial scales including 500-m upstream of each sampling site, 500-m upstream with inverse-distance weighting, and over the integrated upstream watershed (Fig. 2A–C). A range of spatial scales has been used previously to examine correlations between PAHs and surrounding land use. For instance, Comeleo et al. (1996) reported that the amount of developed land located within 10 km of a sampling

**Table 2**
Land use/land cover site characteristics.

| | 500-m upstream buffer | | | | | | 500-m upstream buffer (IDW) | | | | | | Integrated upstream watershed | | | | | |
|---|---|---|---|---|---|---|---|---|---|---|---|---|---|---|---|---|---|---|
| Site# | IMP | CIR | RES | URB | RESCI | RDS | IMP | CIR | RES | URB | RESCI | RDS | IMP | CIR | RES | URB | RESCI | RDS |
| 0 | 0.3 | 0.0 | 0.0 | 0.0 | 0.0 | 0.0 | 11.7 | 0.0 | 0.0 | 0.0 | 0.0 | 0.0 | 0.1 | 0.0 | 0.0 | 0.0 | 0.0 | 0.0 |
| 1 | 0.4 | 0.0 | 0.0 | 0.0 | 0.0 | 0.0 | 29.1 | 0.0 | 0.0 | 0.0 | 0.0 | 0.0 | 0.1 | 0.0 | 0.0 | 0.0 | 0.0 | 0.0 |
| 2 | 0.3 | 0.0 | 0.0 | 0.0 | 0.0 | 0.0 | 35.0 | 0.0 | 0.0 | 0.0 | 0.0 | 0.0 | 0.1 | 0.0 | 0.0 | 0.0 | 0.0 | 0.0 |
| 3 | 0.9 | 0.0 | 0.0 | 0.0 | 0.0 | 0.0 | 81.7 | 0.0 | 0.0 | 0.0 | 0.0 | 0.0 | 0.1 | 0.0 | 0.0 | 0.0 | 0.0 | 0.0 |
| 4 | 0.2 | 0.0 | 0.0 | 0.0 | 0.0 | 0.0 | 6.4 | 0.0 | 0.0 | 0.0 | 0.0 | 0.0 | 0.1 | 0.0 | 0.0 | 0.0 | 0.0 | 0.0 |
| 5 | 9.9 | 16.5 | 19.6 | 36.1 | 25.1 | 11.0 | 498.1 | 12.8 | 7.6 | 20.5 | 13.2 | 7.3 | 0.2 | 0.8 | 0.2 | 0.9 | 0.3 | 0.7 |
| 6 | 0.5 | 0.0 | 0.0 | 0.0 | 0.0 | 0.0 | 16.3 | 0.0 | 0.0 | 0.0 | 0.0 | 0.0 | 0.3 | 6.1 | 6.5 | 12.6 | 9.3 | 3.3 |
| 7 | 3.0 | 4.1 | 12.2 | 16.3 | 12.2 | 4.1 | 190.3 | 1.8 | 5.1 | 6.9 | 5.1 | 1.8 | 0.4 | 2.8 | 1.7 | 4.5 | 2.6 | 1.8 |
| 8 | 0.8 | 5.4 | 10.1 | 15.5 | 10.1 | 5.4 | 36.1 | 2.3 | 4.0 | 6.3 | 4.0 | 2.3 | 1.8 | 17.7 | 4.2 | 22.0 | 20.4 | 1.5 |
| 9 | 1.5 | 2.3 | 5.5 | 7.8 | 7.8 | 0.0 | 75.3 | 0.8 | 2.1 | 2.9 | 2.9 | 0.0 | 1.8 | 2.2 | 5.8 | 8.0 | 8.0 | 0.0 |
| 10 | 0.5 | 0.0 | 0.0 | 0.0 | 0.0 | 0.0 | 33.3 | 0.0 | 0.0 | 0.0 | 0.0 | 0.0 | 2.2 | 3.7 | 5.3 | 9.0 | 7.2 | 1.8 |
| 11 | 0.6 | 1.8 | 10.4 | 12.2 | 10.4 | 1.8 | 28.6 | 0.5 | 3.0 | 3.5 | 3.0 | 0.5 | 2.1 | 2.1 | 1.3 | 3.4 | 1.6 | 1.8 |
| 12 | 1.6 | 1.6 | 0.0 | 1.6 | 0.0 | 1.6 | 59.0 | 1.4 | 0.0 | 1.4 | 0.0 | 1.4 | 2.0 | 4.6 | 2.6 | 7.1 | 4.0 | 3.1 |
| 13 | 1.4 | 0.0 | 0.0 | 0.0 | 0.0 | 0.0 | 98.0 | 0.0 | 0.0 | 0.0 | 0.0 | 0.0 | 2.0 | 3.1 | 4.1 | 7.2 | 5.0 | 2.2 |
| 14 | 1.6 | 9.1 | 1.1 | 10.3 | 1.1 | 9.1 | 133.6 | 8.2 | 0.6 | 8.8 | 0.6 | 8.2 | 2.0 | 3.0 | 2.7 | 5.7 | 3.3 | 2.4 |
| 15 | 4.4 | 8.7 | 0.0 | 8.7 | 8.7 | 0.0 | 295.2 | 4.4 | 0.0 | 4.4 | 4.4 | 0.0 | 1.9 | 1.8 | 3.1 | 4.9 | 3.5 | 1.4 |
| 16 | 0.8 | 0.0 | 0.0 | 0.0 | 0.0 | 0.0 | 29.1 | 0.0 | 0.0 | 0.0 | 0.0 | 0.0 | 1.9 | 2.7 | 5.5 | 8.2 | 6.3 | 1.9 |
| 17 | 5.5 | 10.9 | 33.2 | 44.1 | 33.2 | 10.9 | 103.2 | 1.8 | 5.1 | 6.9 | 5.1 | 1.8 | 2.1 | 8.9 | 10.1 | 19.0 | 15.9 | 3.1 |
| 18 | 0.1 | 1.9 | 0.0 | 1.9 | 0.0 | 1.9 | 1.8 | 0.7 | 0.0 | 0.7 | 0.0 | 0.7 | 2.2 | 4.7 | 9.8 | 14.4 | 12.0 | 2.4 |
| 19 | 24.7 | 34.1 | 41.7 | 75.8 | 66.4 | 9.3 | 934.9 | 17.4 | 13.6 | 31.1 | 27.2 | 3.9 | 2.3 | 6.0 | 19.5 | 25.5 | 23.5 | 2.0 |
| 20 | 12.1 | 18.1 | 9.7 | 27.9 | 27.9 | 0.0 | 800.1 | 11.3 | 6.3 | 17.5 | 17.5 | 0.0 | 2.4 | 2.2 | 9.7 | 11.9 | 10.7 | 1.2 |
| 21 | 32.7 | 43.8 | 26.0 | 69.8 | 59.6 | 10.1 | 2077.2 | 27.4 | 15.2 | 42.6 | 36.6 | 6.0 | 3.1 | 22.2 | 17.3 | 39.4 | 34.2 | 5.2 |
| 22 | 29.5 | 5.9 | 0.0 | 5.9 | 5.4 | 0.5 | 286.6 | 6.6 | 0.0 | 6.6 | 6.4 | 0.2 | 3.1 | 41.8 | 0.0 | 41.8 | 41.8 | 0.0 |
| 23 | 14.6 | 0.0 | 29.9 | 29.9 | 29.9 | 0.0 | 335.3 | 0.0 | 6.3 | 6.3 | 6.3 | 0.0 | 3.1 | 2.1 | 5.6 | 7.7 | 6.3 | 1.5 |
| 24 | 4.4 | 11.1 | 26.0 | 37.1 | 26.0 | 11.1 | 188.2 | 4.4 | 10.9 | 15.2 | 10.9 | 4.4 | 3.1 | 4.9 | 11.0 | 15.9 | 12.8 | 3.1 |
| 25 | 10.2 | 0.0 | 18.6 | 18.6 | 18.6 | 0.0 | 475.7 | 0.0 | 10.2 | 10.2 | 10.2 | 0.0 | 3.1 | 3.4 | 13.4 | 16.8 | 13.6 | 3.1 |
| 26 | 20.0 | 32.0 | 7.2 | 39.2 | 24.1 | 15.1 | 670.6 | 10.3 | 2.9 | 13.2 | 8.5 | 4.8 | 3.8 | 13.9 | 16.2 | 30.0 | 26.1 | 3.9 |
| 28 | 15.5 | 3.9 | 71.7 | 75.6 | 71.7 | 3.9 | 777.4 | 2.2 | 38.9 | 41.0 | 38.9 | 2.2 | 3.9 | 6.8 | 40.5 | 47.3 | 40.9 | 6.3 |
| 29 | 18.2 | 11.3 | 55.7 | 67.0 | 55.7 | 11.3 | 814.3 | 6.7 | 23.2 | 29.9 | 23.2 | 6.7 | 3.9 | 9.8 | 46.3 | 56.0 | 47.5 | 8.6 |
| 30 | 15.9 | 5.8 | 66.6 | 72.4 | 66.6 | 5.8 | 596.0 | 2.8 | 25.9 | 28.7 | 25.9 | 2.8 | 4.0 | 10.8 | 29.5 | 40.3 | 36.3 | 4.0 |
| 31 | 11.3 | 11.3 | 27.8 | 39.1 | 27.8 | 11.3 | 369.5 | 3.7 | 7.3 | 11.0 | 7.3 | 3.7 | 4.0 | 12.6 | 57.5 | 70.1 | 64.3 | 5.8 |
| 32 | 9.9 | 11.6 | 19.5 | 31.1 | 19.5 | 11.6 | 562.3 | 6.6 | 10.3 | 16.9 | 10.3 | 6.6 | 4.1 | 5.6 | 34.7 | 40.2 | 35.6 | 4.6 |
| 33 | 15.4 | 11.0 | 49.4 | 60.4 | 53.9 | 6.5 | 796.7 | 7.2 | 21.7 | 28.9 | 23.2 | 5.7 | 4.2 | 8.4 | 54.9 | 63.3 | 57.8 | 5.5 |
| 34 | 26.6 | 0.4 | 61.4 | 61.8 | 61.4 | 0.4 | 916.9 | 0.1 | 20.6 | 20.7 | 20.6 | 0.1 | 4.3 | 14.2 | 46.2 | 60.4 | 55.0 | 5.4 |
| 35 | 10.5 | 3.9 | 26.3 | 30.2 | 26.7 | 3.5 | 313.0 | 3.2 | 7.1 | 10.3 | 7.2 | 3.1 | 4.3 | 18.6 | 56.5 | 75.1 | 74.2 | 0.9 |

Impervious surface area (IMP) = land cover attributed to impervious surface.
Commercial/Industrial & Roads (CIR) = land use % attributed to ∑low, mid- and high-commercial and industrial activities, and state roads; Residential (RES) = land use % attributed to ∑low, mid- and high-residential areas; Urban (URB) = land use % attributed to ∑Commercial/Industrial & Roads + Residential land use; Residential + Commercial/Industrial (RESCI) = land use % attributed to ∑Commercial/Industrial + Residential (i.e. same as Urban without Roads); Roads (RDS) = land use % attributed to state roads.
Urban (URB) = land use % attributed to ∑Commercial/Industrial & Roads + Residential land use.
Residential + Commercial/Industrial (RESCI) = land use % attributed to ∑Commercial/Industrial + Residential (i.e. same as Urban without Roads); Roads (RDS) = land use % attributed to state roads.

station was a major contributing factor explaining sediment PAH concentrations for 25 Chesapeake Bay sub-estuaries. Crosbie and Chow-Fraser (1999) showed that PAHs in Ontario marsh sediments were correlated with urban land in watersheds ranging in size from 0.10 to 20 $km^2$. More recently, Augusto et al. (2011) showed strong correlations between urban land use and PAHs measured in aquatic mosses transplanted to serve as water pollution bio-monitors in Lisbon, Portugal. That study also demonstrated correlation between total PAHs and four land-use metrics varied depending on the spatial scale used for analysis, and found that the highest correlations were observed at spatial scales ranging from 500 to 1000 m.

Land use/land cover became increasingly more urban, as evidenced by the increased percentage of impervious surface cover, moving eastward along the stream reach (Table 2). Total PAH concentrations ($\sum PAH_{19}$) similarly increased with greater impervious surface cover at all three spatial scales (Fig. 3A–C). This increase is not unexpected given the well-documented relationship between urban PAH sediment concentrations and surface runoff (Hoffman et al., 1984). However, the source of PAHs in urban runoff varies, so we next focused on investigating which urban land-use metrics best correlated with enhanced PAH sediment concentrations.

### 3.2. PAH/land-use correlations

Pairwise rank correlations were performed to investigate the association between six urban land-use/land-cover metrics and $\sum PAH_{12}$ sediment concentrations. Highly significant positive correlations ($p$-value $< 0.0001$) were found for three urban land-use metrics (RES, RESCI, and URB), impervious surface area (IMP), and $\Sigma EPA_{12}$ PAH concentrations at three spatial scales using Spearman's rank correlation analysis (Table 3). Impervious surface cover was highly correlated with total PAHs at all spatial scales ($\rho = 0.68–0.78$, $p = <0.0001$), supporting the hypothesis that urban runoff is a major transport pathway for PAHs in this watershed. Residential and commercial/industrial land use (RESCI) and urban land use (URB) also strongly correlated with PAH concentrations at all spatial scales ($\rho = 0.69–0.81$, $p = <0.0001$), as did residential (RES) land use ($\rho = 0.66–0.69$, $p = <0.0001$). Interestingly, neither roads (RDS) nor the combination of roads with commercial/industrial land (CIR) showed significant correlations with sediment PAH concentrations except at the integrated upstream watershed scale ($\rho = 0.81$, $p = <0.0001$). Similar although weaker trends were observed for the correlations between PAH concentrations and impervious surface, urban land, and the combination of residential and commercial/industrial land use using Pearson's correlation coefficient.

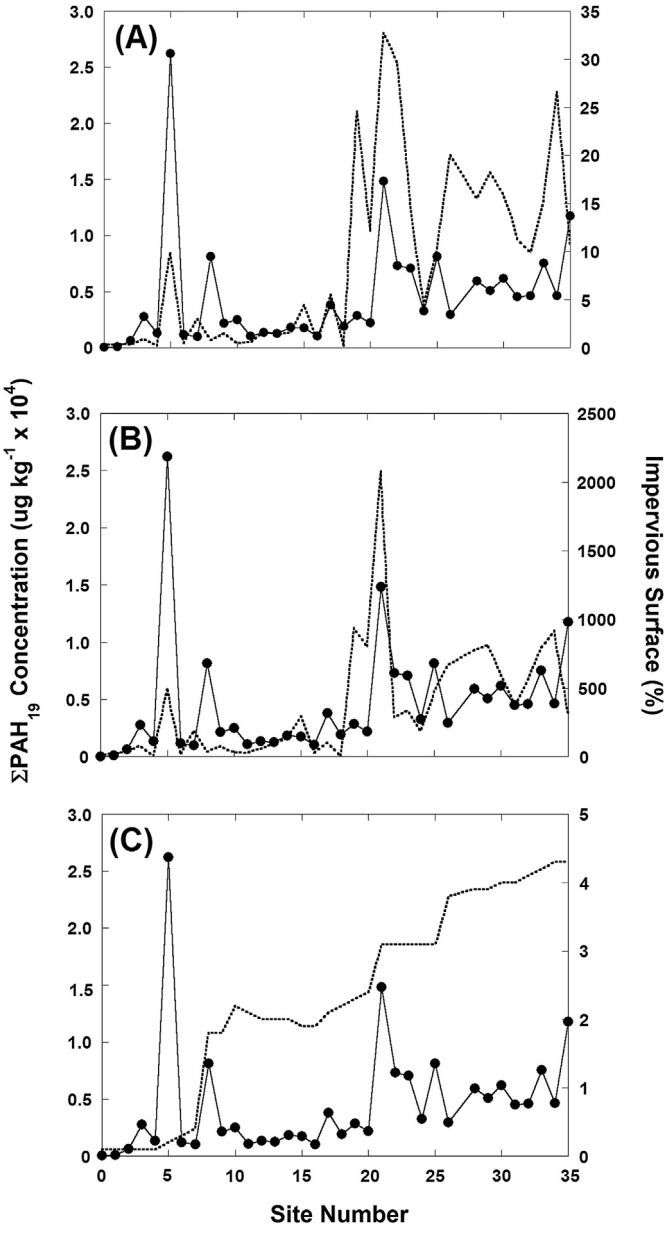


**Fig. 3.** Comparison of $\sum PAH_{19}$ concentrations (depicted by closed circles from left to right along *x*-axis, representing site numbers from west to east in watershed) with impervious surface area % (depicted as a dotted line) at three spatial scales. (A) 500-m upstream buffer; (B) 500-m inverse-distance-weighted (IDW) upstream buffer; and (C) integrated upstream watershed area.

If PAH sources are linked to human activities taking place on urban land, then increasing the percentage of that land-use/land-cover type within a watershed might reasonably be predicted to result in increased PAH concentrations (Chalmers et al., 2007). Conversely, if no correlation is observed between a specified land-use and PAH concentrations, then the activities taking place there should have a minimal influence on sediment PAH concentrations. The strong and highly significant correlations between IMP, RES, RESCI, URB land and $\sum PAH_{12}$ observed in this study suggest that a shared feature in common between these land-use/land-cover types influences sediment PAH concentrations in this watershed.

A newly identified PAH source in the environment is coal-tar-based sealcoat, a major source of PAHs to Austin, TX stream sediments (Mahler et al., 2005) and to urban lakes located in the eastern U.S. (Van Metre et al., 2009). Yang et al. (2010) showed that carbonaceous particles containing coal-tar pitch, which is used in some types of sealcoat, serve as the dominant source of PAHs to commercial soils, lake sediments, sealed parking lots, and streambed sediments in Fort Worth, TX. Watts et al. (2010) measured 24-fold increases in New Hampshire sediments receiving storm water runoff from parking lots after coal-tar-based sealant was applied. Banger et al. (2010) measured PAHs in urban soils from Miami, FL collected from different depths and found that surface (0–15 cm) soils contained higher PAH concentrations than those collected at depth (30–45 cm), and that soils collected from commercial land-use areas had higher PAH concentrations than those from public parks, public buildings, or residential areas. This evidence, considered collectively, supports the hypothesis that coal-tar-based sealcoat is an important recent PAH source to surface sediments in this watershed because individuals and businesses often apply sealcoat to privately-owned impervious surface cover (such as driveways and parking lots) to maintain durability, and these activities occur primarily in areas with high residential and commercial/industrial land use.

Conversely, the lack of a correlation between sediment PAH concentrations and roads is striking, given that roads are 100% impervious surface cover. However, public roads are not commonly sealcoated. Thus, our data suggests that human activities associated with roads (i.e. vehicle emissions) are a less important PAH source to surface sediments in this watershed, and may reflect the approximate 15–>30-fold declines in vehicle emission factors since the 1970s (Beyea et al., 2008; Shen et al., 2011).

Land-use/sediment PAH correlation coefficients generally improved as the spatial scale increased from the local scale (e.g. 500-m) to the catchment scale (e.g. integrated upstream watershed), and were consistently significant for the same urban land use/land cover categories (i.e. IMP, RES, URB, and RESCI) at all spatial scales (Table 3). In contrast, inverse-distance weighting (IDW) only moderately improved correlation coefficients between PAHs and urban land-use categories, suggesting that land-use pattern was less important than land-use type in explaining the correlations at small spatial scales. The IDW results in this study are similar to those of Scoggins et al. (2007) who found that neither the total area of coal-tar-sealed parking lot nor its proximity to the sampling site were significantly correlated with PAH sediment concentrations in Austin, TX urban streams.

The improved correlations between $\sum PAH_{12}$ and land-use/land-cover metrics observed with increased spatial scale imply that upstream land-use/land-cover activities impact watershed sediment quality at large spatial scales, similar to results reported by Van Dolah et al. (2008) for estuarine PAHs located in South Carolina coastal zones. The fact that PAH sediment concentrations better reflect land-use/land-cover at the catchment versus local scale is surprising, and suggests that PAHs in coal-tar-based sealcoat may be more mobile than PAHs from other sources. Interestingly, previous research has demonstrated that offsite transport of PAH-contaminated dust from coal-tar-based sealcoated parking lots to unsealed lots occurs, either through wind action, vehicle tracking, or snow removal (Van Metre et al., 2009). Whether or not one or more of these factors are important for explaining the data reported here are unknown. In this study, two of the three spatial scales examined were highly correlated with each other (i.e. the 500-m upstream buffer and the 500-m IDW upstream buffer) while the integrated upstream watershed scale showed no correlation to the local buffer scales. These results, taken together, suggest that using both a local and catchment-size spatial scale in a GIS analysis can provide complementary and potentially useful information on PAH sources.

**Table 3**
Correlations between $\sum EPA_{12}$ PAH concentrations in streambed sediments ($n = 34$) and urban land-use/land-cover (LULC) metrics at three spatial scales.

| A. Spearman's rank | | 500-m upstream buffer | | Inverse-distance weighted 500-m upstream buffer | | Integrated upstream watershed | |
|---|---|---|---|---|---|---|---|
| Land use/land cover (%) | Abbr | $\rho$ | $p$-Value | $\rho$ | $p$-Value | $\rho$ | $p$-Value |
| Impervious surface | IMP | **0.73** | **<0.0001** | **0.68** | **<0.0001** | **0.78** | **<0.0001** |
| Commercial/Industrial & Roads | CIR | 0.45 | 0.0077 | 0.47 | 0.0053 | **0.81** | **<0.0001** |
| Residential | RES | **0.66** | **<0.0001** | **0.69** | **<0.0001** | **0.67** | **<0.0001** |
| Urban | URB | **0.69** | **<0.0001** | **0.70** | **<0.0001** | **0.81** | **<0.0001** |
| Residential & Commercial/Industrial | RESCI | **0.69** | **<0.0001** | **0.73** | **<0.0001** | **0.81** | **<0.0001** |
| Roads | RDS | 0.45 | 0.0077 | 0.49 | 0.0036 | 0.45 | 0.0072 |
| B. Pearson's $r$ on concentration | | 500-m upstream buffer | | Inverse-distance weighted 500-m upstream buffer | | Integrated upstream watershed | |
| Land use/land cover (%) | | $r$ | $p$-Value | $r$ | $p$-Value | $r$ | $p$-Value |
| Impervious surface | IMP | **0.66** | **<0.0001** | **0.66** | **<0.0001** | **0.64** | **<0.0001** |
| Commercial/Industrial & Roads | CIR | 0.40 | 0.0191 | 0.49 | 0.0034 | **0.65** | **<0.0001** |
| Residential | RES | 0.49 | 0.0035 | 0.49 | 0.0031 | 0.52 | 0.0015 |
| Urban | URB | 0.56 | 0.0005 | 0.61 | 0.0001 | **0.67** | **<0.0001** |
| Residential & Commercial/Industrial | RESCI | 0.56 | 0.0005 | 0.59 | 0.0002 | **0.68** | **<0.0001** |
| Roads | RDS | *0.30* | *0.0830* | *0.39* | *0.0236* | *0.37* | *0.0297* |

Highly significant relations at $p$-value < 0.0001 are shown in bold. Correlations that are not significant ($p > 0.01$) are in italic. Sites are characterized by varying percentages of urban land uses: Commercial/Industrial & Roads (CIR) = land use % attributed to ∑low-, mid- and high-commercial and industrial activities, and state roads; Residential (RES) = land use % attributed to ∑low-, mid- and high-residential areas; Urban (URB) = land use % attributed to ∑Commercial/Industrial & Roads + Residential land use; Residential + Commercial/Industrial (RESCI) = land use % attributed to ∑Commercial/Industrial + Residential (i.e. same as Urban without Roads); Roads (RDS) = land use % attributed to state roads.

### 3.3. Distinguishing urban from rural sediments using principal components analysis (PCA)

Because multiple PAH sources can originate from the same type of land use, we used principal components analysis (PCA) to group sediments with similar chemical variances in order to identify potential PAH sources. The purpose of using PCA in this study is to simplify the interpretation of similarities and differences among samples by reducing the number of variables, while still explaining most of the variance.

Fractional PAH concentrations for 32 sediment samples were submitted to PCA which resulted in the first two principal components accounting for 86% of the observed variance in the sediment data (Fig. 4). In PCA, the spatial relationship(s) between sampling sites (denoted by site number) are representative of the chemical relationship between samples; the closer two sites are to each other the more similar the sediment chemistry. The intersection of the dotted lines in the bi-plot represents the variance of an average sample; the farther the distance from the origin each site lies, the more unique its sediment chemistry.

As observed in Fig. 4, two trends are apparent. First, principal component 1 (PC1), which explains 75% of the sample variance, effectively separates 'rural' from 'urban' sediments because 'rural' sites lie to the right of the origin line while urban sites lie to the left. The underlying chemical explanation for the delineation is revealed by the factor loadings. Factor loadings on PC1 show that rural samples are enriched in benzofluoranthene isomers (BkF, BbF) and BeP compared to urban sites, which are enriched in Anth, Phe, Fla, Py, Chry, BaA, BaP, Ip and BghiP. Furthermore, the spread observed in the principal component data indicates that more than one rural PAH source may be important, typical of atmospheric combustion sources.

Conversely, principal component 2 (PC2) accounts for 11% of the sample variance, and moderately separates 'urban' sites into those that are enriched in high-molecular weight PAHs such as Ip and BghiP (along with BaP; upper left quadrant in Fig. 4) from those containing Anth, Phe, Fla, Py, Chry, BaA (lower left quadrant). The proximity of the urban principal component data to each other suggests that a single dominant PAH source or multiple PAH sources with similar source strengths and chemical assemblages are important in explaining urban PAH profiles. To further identify PAH sources associated with various land-use activities, we focused on comparing sediment PAH assemblages from rural and urban areas to known PAH source assemblages using Chi-square and Pearson correlation analysis.

### 3.4. Identifying urban and rural PAH sources using fractional PAH assemblages

An average urban sediment PAH assemblage was calculated based on the mean (±SD) fractional PAH composition for $n = 22$ sediments classified as 'urban' using PCA (e.g. the sites to the left of

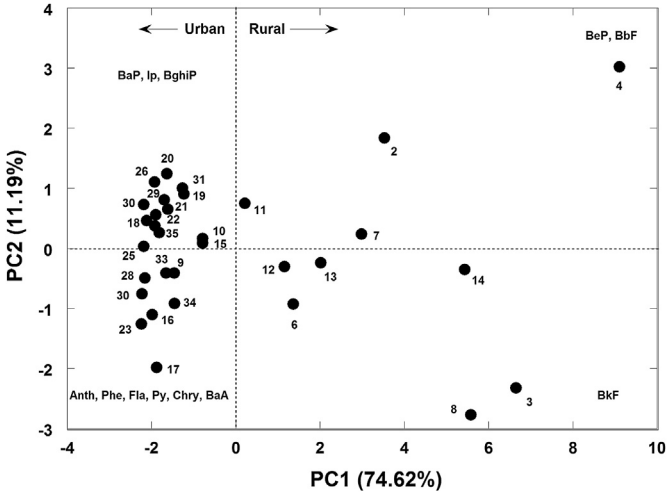


**Fig. 4.** PCA scores/loadings plot for Conodoguinet Creek sediments. The samples cluster as a function of location in the watershed; rural sites (PC1) are enriched in their fractional percentages of BeP, BbF, and BkF relative to urban sites (PC2). The spread in the data suggests that more than one source may be important in rural areas. Urban sites (PC2) are enriched in their fractional percentages of Anth, Phe, Fla, Py, Chry, BaA, BaP, Ip, and BghiP relative to rural sites. The proximity of the data to each other suggests that a single source may be important in urban areas.

the origin line in Fig. 4) and quantitatively compared to known PAH source assemblages (Fig. 5A–G) compiled from published data (Table 4). Chi-square values ($X^2$) were calculated as the sum of the difference in proportional PAH concentrations divided by the mean of the two values, summed for the 12 EPA PAHs; a smaller value of $X^2$ indicates greater similarity between the two profiles (Van Metre and Mahler, 2010). Pearson correlation coefficients ($r$) were also calculated to evaluate the similarities between the average urban sediment profile and individual PAH sources.

The average urban sediment assemblage was quantitatively compared to PAH assemblages from power-plant emissions (Fig. 5A, $X^2 = 0.023$, $r = 0.67$), residential-coal emissions (Fig. 5B, $X^2 = 0.092$, $r = 0.30$), coke-oven emissions (Fig. 5C, $X^2 = 0.020$, $r = 0.30$), gas-engine emissions (Fig. 5D, $X^2 = 0.016$, $r = 0.82$), diesel-engine emissions (Fig. 5E, $X^2 = 0.055$, $r = 0.66$), traffic-tunnel emissions (Fig. 5F, $X^2 = 0.009$, $r = 0.69$), and an average ($n = 47$) coal-tar-based sealcoat dust profile (Fig. 5G, $X^2 = 0.006$, $r = 0.94$). The low Chi-square value ($X^2 = 0.006$) and high Pearson correlation

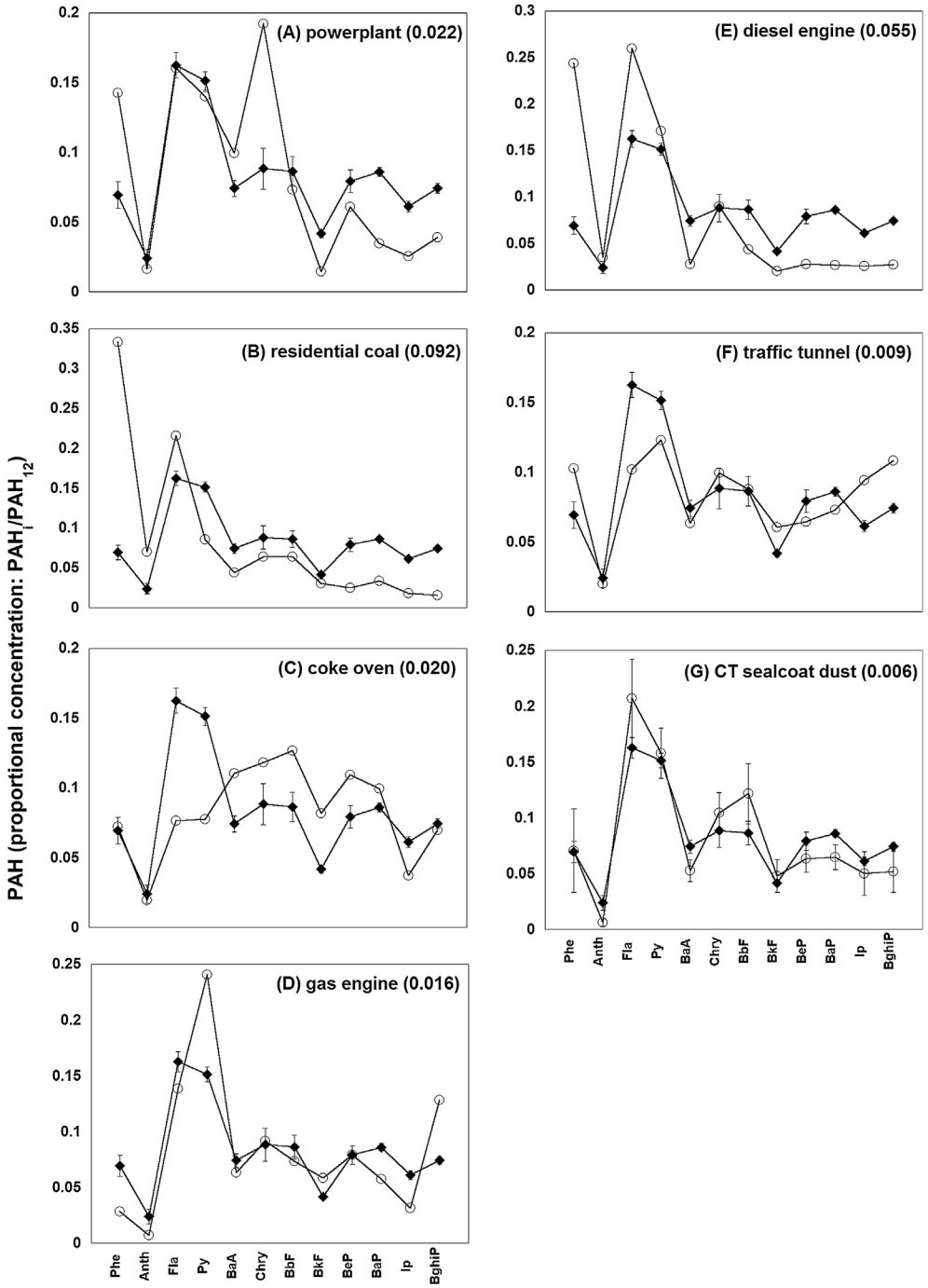


**Fig. 5.** Comparison of PAH profiles (from left to right along $x$-axis, low to high molecular weight) for various PAH sources (○; Table 4) to the mean urban PAH profile ($n = 22$) measured in this study (●; uncertainty bars represent the standard deviation). Chi-square statistic for each comparison is shown in parentheses. (A) power plant coal; (B) residential coal; (C) coke-oven emissions; (D) gas-engine emissions; (E) diesel emissions; (F) traffic-tunnel emissions; and (G) coal-tar-based sealcoat profile ($n = 47$).

**Table 4**
PAH source categories and source profiles.

| Source category | PAH source | *n* | References |
|---|---|---|---|
| Coal combustion | Power plant emissions | 3 | Li et al., 2003 |
| | Residential heating emissions | 3 | Li et al., 2003 |
| | Coke-oven emissions | 5 | Li et al., 2003 |
| Vehicle related | Gas engine particulate emissions | 4 | Li et al., 2003 |
| | Diesel engine particulate emissions | 5 | Li et al., 2003 |
| | Traffic tunnel | 8 | Li et al., 2003 |
| Coal-tar-based sealcoat related | Coal-tar-based sealcoat dust | 8 | Mahler et al., 2004 |
| | Coal-tar-based sealcoat dust | 1 | Yang et al., 2010 |
| | Coal-tar-based sealcoat dust | 11 | Mahler et al., 2010 |
| | Coal-tar-based sealcoat dust, 6 cities | 21 | Van Metre et al., 2008 |
| | Coal-tar-based sealcoat dust | 6 | Van Metre et al., 2012 |

*n* = Number of literature sources compiled to generate profile.

coefficient ($r = 0.94$) observed for the comparison between urban sediments and sealcoat dust (Fig. 5G, $p = <0.0001$) indicates that coal-tar-based sealcoat dust is a significant urban PAH source in the Conodoguinet Creek watershed, similar to results reported previously for 40 U.S. lakes by Van Metre and Mahler (2010).

Because rural fractional PAH assemblages exhibited a higher degree of variability in the PCA data (Fig. 4) relative to urban sites (thus potentially indicating more than one PAH source) we compared rural sites to known PAH source assemblages on a site-by-site basis instead of aggregating the fractional profiles into an average rural PAH assemblage. Ten rural sediment assemblages were compared individually to each of the same seven PAH sources described above for urban sediments using Chi-square and Pearson correlation analysis. Seven of the ten 'rural' sites (e.g. 2, 3, 4, 7, 8, 13, 14) had PAH assemblages that most closely matched the PAH assemblage from coke-oven emissions ($X^2 = 0.017–0.139$, $r = 0.69–0.78$) and three sites (e.g. 6, 11, 12) correlated more closely with coal-tar-based sealcoat dust ($X^2 = 0.012–0.013$, $r = 0.89–0.91$). Consequently, coke-oven-based emissions emerged as an important atmospheric combustion source to sediments collected from the more rural western end of the watershed. As of 2010, Pennsylvania had four coke-oven plants operating in the state, three of which are located approximately 150 miles due west (upwind) of the Conodoguinet Creek headwaters (American Coke and Coal Chemicals Institute, 2010).

## 4. Conclusions

This study demonstrates that coal-tar-based sealcoat is a major PAH source to urbanizing freshwater stream sediments and its occurrence is strongly related to residential and commercial/industrial land use in the Conodoguinet Creek watershed. Principal components analysis chemically differentiated two PAH assemblages along the stream reach. A rural PAH assemblage is chemically enriched in BbF, BkF and BeP relative to other PAH isomers, and is indicative of a coke-oven PAH emission source. The urban PAH assemblage is significantly and highly correlated with surrounding urban land use/land cover metrics, especially impervious surface area, residential and commercial/industrial land (RESCI) and urban land use (URB). Chi-square and Pearson correlation analyses revealed strong similarities between urban sediment assemblages and coal-tar-based sealcoat dust, and between rural sediment assemblages and coke-oven-based combustion emissions. Taken collectively, these results strongly suggest that coal-tar-based sealcoat is an important urban PAH source in the Conodoguinet Creek watershed, consistent with other studies that have recently identified coal-tar-based sealcoat as the primary cause of upward trends in PAH concentrations due to increasing urban sprawl. These results also suggest that human activities associated with residential and commercial/industrial land use where coal-tar-based sealcoat is present influence watershed health at large spatial scales. From a regulatory standpoint, this work implies that protection of local water supplies and sediment resources may be best served through targeted citizen education about the possible unintended consequences of coal-tar-based sealcoat use.

## Acknowledgments

We thank Scott Mabury, Emma Goosey, and Miriam Diamond at the University of Toronto for facilitating the sediment extraction, and Jim Ciarocca and Kristin Brubaker for help with the GIS analyses. We also thank the anonymous reviewers whose comments greatly strengthened the original manuscript. Dickinson College Research and Development Grants supported this work and were awarded to AEW, SB and MN. The GC–MS used in this work was supported through funding awarded to Dickinson College by the Sherman-Fairchild Foundation.

## Appendix A. Supplementary data

Supplementary data related to this article can be found at http://dx.doi.org/10.1016/j.envpol.2013.10.015.

## References

Alliance for the Chesapeake Bay, Conodoguinet Creek Fact Sheet, 1994. Available from: https://allianceforthebay.org/resources/publications-old/pennsylvania-river-fact-sheet/, (accessed October 2013).
American Coke and Coal Chemicals Institute, Operating U.S. Coke Plants List, 2010. Available from: http://accci.org/documents/CokePlantListing_010112.pdf, (accessed October 2013).
Augusto, S., Gonzalez, C., Vieira, R., Maguas, C., Branquinho, C., 2011. Evaluating sources of PAHs in urban streams based on land use and biomonitors. Environ. Sci. Technol. 45, 3731–3738.
Banger, K., Toor, G.S., Chirenje, T., Ma, L., 2010. Polycyclic aromatic hydrocarbons in urban soils of different land uses in Miami, FL. Soil Sediment Contam. Int. J. 19, 231–243.
Beyea, J., Stellman, S.D., Hatch, M., Gammon, M.D., 2008. Airborne emissions from 1961 to 2004 of benzo(a)pyrene from U.S. vehicles per km of travel based on tunnel studies. Environ. Sci. Technol. 42, 7315–7320.
Chalmers, A.T., Van Metre, P.C., Callender, E., 2007. The chemical response of particle-associated contaminants in aquatic sediments to urbanization in New England, USA. J. Contam. Hydrol. 91, 4–25.
Comeleo, R.L., Paul, J.F., August, P.V., Copeland, J., Baker, C., Hale, S.S., Latimer, R.W., 1996. Relationships between watershed stressors and sediment contamination in Chesapeake Bay estuaries. Landsc. Ecol. 11 (5), 307–319.
Conover, W.J., Iman, R.L., 1981. Rank transformations as a bridge between parametric and nonparametric statistics. Am. Stat. 35 (3), 124–129.
Crosbie, B., Chow-Fraser, P., 1999. Percentage land use in the watershed determines the water and sediment quality of 22 marshes in the Great Lakes basin. Can. J. Fish Aquat. Sci. 56, 1781–1791.
Dickhut, R.M., Canuel, E.A., Gustafson, K.E., Liu, K., Arzayus, K.M., Walker, S.E., Edgecombe, G., Gaylor, M.O., Macdonald, E.H., 2000. Automotive sources of carcinogenic polycyclic aromatic hydrocarbons associated with particulate matter in the Chesapeake Bay region. Environ. Sci. Technol. 34, 4635–4640.
Hoffman, E.J., Mills, G.L., Latimer, J.S., Quinn, J.G., 1984. Urban runoff as a source of polycyclic aromatic hydrocarbons to coastal waters. Environ. Sci. Technol. 18, 580–587.
Jartun, M., Ottesen, R.T., Steinnes, E., Volden, T., 2008. Runoff of particle bound pollutants from urban impervious surfaces studied by analysis of sediments from stormwater traps. Sci. Total Environ. 396, 147–163.
Li, A., Jang, J.-K., Scheff, P.A., 2003. Application of EPA CMB82 model for source apportionment of sediment PAHs in Lake Calumet, Chicago. Environ. Sci. Technol. 37, 2958–2965.
MacDonald, D.D., Ingersoll, C.G., Berger, T.A., 2000. Development and evaluation of consensus-based sediment quality guidelines for freshwater ecosystems. Arch. Environ. Contam. Toxicol. 39, 20–31.
Mahler, B.J., Van Metre, P.C., Wilson, J.T., 2004 [revised 2007]. Concentrations of Polycyclic Aromatic Hydrocarbons (PAHs) and Major and Trace Elements in Simulated Rainfall Runoff from Parking Lots, Austin, Texas, 2003 (Version 3). U.S. Geological Survey Open-File Report 2004-1208, 87 p. [Online only]; (accessed November 2012).

Mahler, B.J., Van Metre, P.C., Bashara, T.J., Wilson, J.T., Johns, D.A., 2005. Parking lot sealcoat: an unrecognized source of urban polycyclic aromatic hydrocarbons. Environ. Sci. Technol. 39, 5560–5566.

Mahler, B.J., Van Metre, P.C., Wilson, J.T., Musgrove, M.L., 2010. Coat-tar-based parking lot sealcoat: an unrecognized source of PAH to settled house dust. Environ. Sci. Technol. 44, 894–900.

Paul, J.F., Comeleo, R.L., Copeland, J., 2002. Landscape metrics and estuarine sediment contamination in the mid-Atlantic and southern New England regions. J. Environ. Qual. 31, 836–845.

Riva-Murray, K., Riemann, R., Murdoch, P., Fischer, J.M., Brightbill, R., 2010. Landscape characteristics affecting streams in urbanizing regions on the Delaware River Basin (New Jersey, New York, and Pennsylvania, U.S.). Landsc. Ecol. 25, 1489–1503.

Scoggins, M., McClintock, N.L., Gosselink, L., 2007. Occurrence of polycyclic aromatic hydrocarbons below coal-tar-sealed parking lots and effects of stream benthic macroinvertebrate communities. J. N. Am. Benthol. Soc. 26, 694–707.

Shen, H., Tao, S., Wang, R., Wang, B., Shen, G., Li, W., Su, S., Huang, Y., Wang, X., Liu, W., Li, B., Sun, K., 2011. Global time trends in PAH emissions from motor vehicles. Atmos. Environ. 45, 2067–2073.

U.S. Environmental Protection Agency, 1993. Provisional Guidance for Quantitative Risk Assessment of Polycyclic Aromatic Hydrocarbons. US Environ Prot Agency Report EPA/600/R-93/089.

Van Dolah, R.F., Riekerk, G.H.M., Bergquist, D.C., Felber, J., Chestnut, D.E., Holland, A.F., 2008. Estuarine habitat quality reflects urbanization at large spatial scales in South Carolina's coastal zone. Sci. Total Environ. 390, 142–154.

Van Metre, P.C., Mahler, B.J., Wilson, J.T., Burbank, T.L., 2008. Collection and Analysis of Samples for Polycyclic Aromatic Hydrocarbon Analysis in Dust and Other Solids Related to Sealed and Unsealed Pavement From 10 Cities Across the United States, 2005–07. In: U.D. Geological Survey Data Series 361, 5 p.

Van Metre, P.C., Mahler, B.J., Wilson, J.T., 2009. PAHs underfoot: contaminated dust from sealcoated pavements. Environ. Sci. Technol. 43, 20–25.

Van Metre, P.C., Mahler, B.J., 2010. Contribution of PAHs from coal-tar pavement sealcoat and other sources to 40 U.S. lakes. Sci. Total Environ. 409, 334–344.

Van Metre, P.C., Majewski, M.S., Mahler, B.J., Foreman, W.T., Braun, C.L., Wilson, J.T., Burbank, T.L., 2012. PAH volatilization following application of coal-tar-based pavement sealant. Atmos. Environ. 51, 108–115.

Watts, A.W., Ballestero, T.P., Roseen, R.M., Houle, J.P., 2010. Polycyclic aromatic hydrocarbons in stormwater runoff from sealcoated pavements. Environ. Sci. Technol. 44, 8849–8854.

Yang, Y., Van Meter, P.C., Mahler, B.J., Wilson, J.T., Ligouis, B., Rassaque, M.D.H., Schaeffer, D.J., Werth, C.J., 2010. Influence of coal-tar sealcoat and other carbonaceous materials on polycyclic aromatic hydrocarbon loading in an urban watershed. Environ. Sci. Technol. 44, 1217–1223.

Zheng, W., Lichwa, J., Yan, T., 2011. Impact of different land uses on polycyclic aromatic hydrocarbon contamination in coastal stream sediments. Chemosphere 84, 376–382.